Characterization, quantification, and replication of human sinus bone for surgery simulation phantoms

Characterization, quantification, and replication of human sinus bone for surgery simulation phantoms

G J Radley[1], **A Sama**[2], **J Watson**[3], and **R A Harris**[1*]
[1]Wolfson School of Mechanical and Manufacturing Engineering, Loughborough University, Loughborough, Leicestershire, UK
[2]Department of Otolaryngology, Head and Neck Surgery, Queen's Medical Centre University Hospital NHS Trust, Nottingham, UK
[3]Oral and Maxillofacial Surgery, Queen's Medical Centre University Hospital NHS Trust, Nottingham, UK

The manuscript was received on 19 January 2009 and was accepted after revision for publication on 18 May 2009.

DOI: 10.1243/09544119JEIM577

Abstract: The requirement for artificial but realistic, tactile, anatomical models for surgical practice in medical simulation is increasingly evident and shows potential for greater efficiency and availability, and lower costs. Anatomically correct, detailed models with the physical surgical characteristics of real tissue, combined with the ability to reproduce one-off cases, would provide an invaluable tool in the development of surgery.

This research work investigates the capture of geometrical and physical data from the human sinus to subsequently direct the production and optimization of such simulation phantoms. Micro-computed tomography analysis of the entire sinus was performed to characterize the sinus complex geometry. Following an extensive review, specialized mechanical testing apparatus and methods relevant to the surgical methods employed were designed and produced. This provided comparative analysis methods for both biological and artificial phantom materials and allowed the optimization of phantom materials with respect to the derived target values.

Keywords: surgery simulation, otorhinolarynology, sinus bone, micro-computed tomography, three-dimensional printing

1 INTRODUCTION

In order to justify the work conducted in this project, it is necessary to provide an overview of the associated dangers faced by patients during minimal access surgery (MAS) in the sinus complex (endoscopic sinus surgery). This includes damage to the eye and optic nerve, which lies in the lateral wall of the ethmoid and sphenoid sinus. The sinus roof is composed of a thin layer of bone, only 0.2 mm thick in certain parts, that can easily be penetrated or damaged. Rupturing of the cerebral plate can lead to leakage of cerebral spinal fluid (CSF), which can result in an increased risk of contracting meningitis. Other complications include damage to a number of major arteries, such as the carotid and sphenopalatine artery.

Currently, physical pre-operative simulation and teaching is primarily limited to the use of cadavers and simple models that lack geometric and/or material similarity, or the ability to represent a given clinical condition. The implications of these restrictions to patient safety and the associated costs and procedures involved in their use present a strong case for alternative methods. Suitable models would be invaluable for the evaluation and validation of specific complex cases and also for use as teaching aids.

Relevant data capture is provided by medical image-based modelling, such as computed tomography (CT) and magnetic resonance imaging (MRI). These procedures are widely available in the healthcare system and are routinely employed irrespective

*Corresponding author: Wolfson School of Mechanical and Manufacturing Engineering, Loughborough University, Ashby Road, Loughborough, Leicestershire, LE11 3TU, UK.
email: R.A.Harris@lboro.ac.uk

of physical representations being produced. These imaging data can be converted into a format that allows their automated production as a three-dimensional (3D) physical representation. This involves conversion from digital imaging and communications in medicine (DICOM) data into surface tessellation language (STL) format, then produced by rapid prototyping (RP) systems. This requires the application of threshold values to the cross-sectional images to provide selective isolation of materials of key densities, on which the RP model will be based [**1**, **2**].

The term '3D printing' (3DP) can be synonymous with multiple RP processes. In this report, however, the name is used to refer to a RP process based on the deposition of a liquid binder substance on to a powder build material, as used by Z Corporation (3DP machine producers, Massachusetts, USA) [**3**]. This process can utilize a variety of powder-based materials, the most common of which is an engineered gypsum. The gypsum material was of primary focus for this project owing to its favourable composition to bone. Parts can be used in their 'raw' or 'green' state although more robust models require suitable post-processing techniques [**4**]. The use of a powder-based material produces porous parts, which allow an extensive range of post-process materials to be infiltrated, resulting in a variety of different mechanical and tactile properties. Figure 1 shows a 3DP model of the human sinus, constructed from CT scan data.

Through the combined efforts of a number of researchers at Loughborough University and Queen's Medical Centre (QMC) University Hospital Nottingham, the aim of creating realistic three-dimensional surgical practice phantoms of the human sinus is being explored through the combination of clinical, materials, and process research. Re-creation of the geometry, mechanical properties, and cutting characteristics of the human sinus is the focus of this work. The physical properties of sinus bone are vastly different to other bone found in the body and also vary throughout the sinus complex. The following work is aimed at accurately quantifying the physical properties of sinus bone, enabling precise replication of cutting characteristics and tactile feedback using 3DP technology.

Fig. 1 3DP model of human sinus

2 METHODOLOGY

2.1 Imaging of the human sinus

Characterization of the human sinus using CT imaging is common practice in many ear, nose, and throat (ENT) departments worldwide for planning of surgical procedures. High-resolution CT allows imaging of some trabecular bone geometry in humans. However, spatial resolution is limited to 100–200 μm in order to keep the radiation dose to a tolerable level [**5**]. Although this resolution is sufficient to determine topological properties, it is not possible to quantify structural indices such as trabecular thickness, nor to visualize intricate structures, such as those present in the inner ear [**6**] and the sinus. In this work, CT analysis was conducted to aid the identification and measurement of tissue type and bone structure throughout the sinus complex. This information could then be used to guide 3DP specimen design and influence the material selection and infiltration techniques.

Computed tomography imaging was conducted using a fresh frozen cadaver which provided an otherwise healthy representation of the sinus complex. This was conducted between Queen's Medical Centre and Nottingham City Hospitals with ethical approval.

High exposure clinical spiral CT was used to initially characterize the cadaver sinus, which resulted in improved resolution in the resultant images compared with the conventional dosage. Regions between the mucosa layer and bone, however, were still poorly defined and not ideal for 3D reconstruction using threshold techniques.

Subsequently, the high-dosage clinical CT was deemed to provide insufficient resolution to image intricate bone structures at a suitable level for this project. The requirement for higher resolution promoted the potential suitability of micro-CT (μCT). Prior to μCT analysis of the fresh frozen cadaver specimen, it was sectioned into a block that retained the entire sinus complex while providing a sample size suitable for the μCT apparatus. Comparative

Fig. 2 High-dosage clinical spiral CT slice image

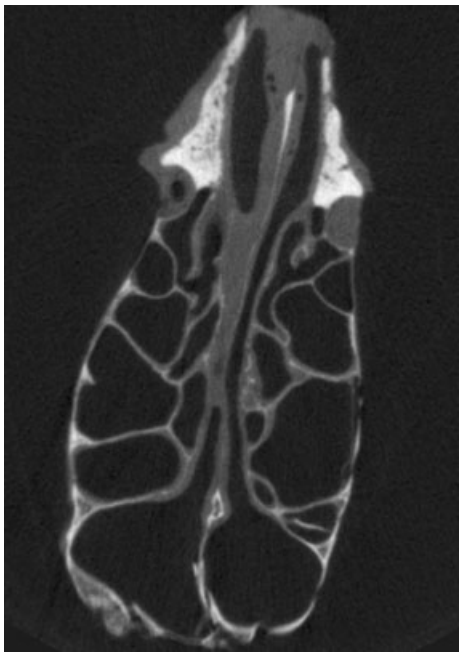

Fig. 3 μCT slice image

images taken from both CT formats are shown in Figs 2 and 3.

Materialise Mimics software (Leuven, Belgium) was then used to convert and view the 'Digital imaging and communications in medicine' (DICOM) data. The subsequent images provide different grey contrasts for different structures, e.g. bone is lighter or soft tissue darker. These different grey contrasts or thresholds have a value. The different image thresholds can be extracted to derive a series of three-dimensional models representing informed tissue variation. These models can be integrated, as shown in Fig. 4, to enable 3D exploration of the human sinus using any CAD program.

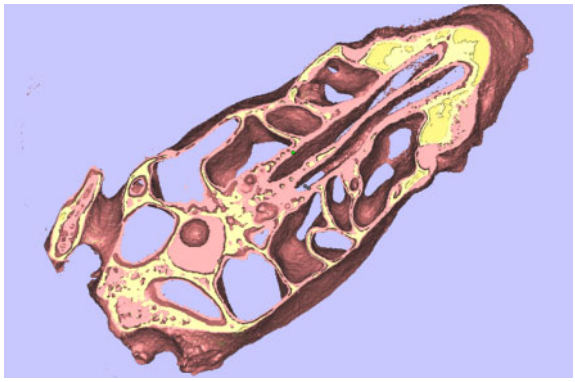

Fig. 4 Integrated reconstruction of sectioned ethmoid and sphenoid complexes

2.2 Mechanical testing of sinus bone

For successful re-creation of the cutting characteristics of human bone using 3DP materials and processes, a suitable methodology for comparative quantification had to be established. A series of conventional mechanical testing procedures were identified and their suitability for testing of small-scale anisotropic samples was assessed. A summary of each methodology and their associated advantages and disadvantages are shown in Table 1.

The problem is compounded by the fact that samples harvested from certain areas of the sinus, such as the ethmoid complex, are extremely small anisotropic structures, typically between 0.1 and 1 mm thick. Post-machining operations on harvested bone samples, to conform with specimen geometry required by conventional processes, would be difficult owing to size restrictions and would also disrupt the native properties of the bone samples. Four-point bending tests have been conducted on very small bone specimens of 7 mm length, using a customized adjustable jig for sample holding [**13**]. However, these tests rely on longitudinal specimens harvested from larger cortical bone to ensure equal stress distribution throughout the sample. Anisotropic bone samples taken from the ethmoid complex would not be able to satisfy this requirement.

In conclusion, the replication and measurement of cutting forces through the use conventional mechanical testing equipment was unsuitable for this project and therefore an alternative method was sought.

2.3 Direct force measurement concept

Previous research has shown that direct measurement of applied forces can be achieved in a variety of

Table 1 Mechanical testing process suitability summary

Mechanical testing method	Specimen preparation requirements	Advantages	Disadvantages	Conclusion	References
Micro-indentation	• Minimal – cleaning • Can be tested hydrated of dehydrated • No premachining	• Suitable for small samples • Minimal bespoke equipment required • Good for comparison of hardness values in a range of areas	• Only provides hardness values for single points • Requires multiple tests to substantiate results • Not suitable for assessing the role of internal structures	*Unsuitable for mechanical analysis of specimens, due to possibility of internal structures and anisotropic nature of sinus bone*	[**7**] [**8**] [**9**]
Tensile testing	• Extensive machining • Samples must be geometrically consistent • Requires a diameter of at least 3-5 mm	• Very accurate method for measuring bone • Loads/displacements can be measured to a high degree of accuracy	• Typically only used for homogeneous specimens with uniform geometries • Small specimens harvested from larger bones to achieve geometrical requirements	*Unsuitable for mechanical analysis of specimens, due to sample size limitations and anisotropic nature of sinus bone*	[**7**] [**10**] [**11**] [**12**]
Compressive testing	• Samples must be machined into cube sections, or whole bones capable of being held	• Test equipment relatively simple • Loads/displacements can be obtained easily	• Not as accurate as tensile tests owing to friction and compression-platen effects • Premature failure can occur owing to poor machining	*Unsuitable for mechanical analysis of specimens, owing to sample size limitations and anisotropic nature of sinus bone*	[**8**] [**9**] [**13**]
3/4-point bend tests	• Samples typically either long bones (femur) or machined specimens harvested from larger samples	• Most similar to mechanical action of surgical tools • Reliable method for determining a range of mechanical properties, such as strength, work to failure, stiffness and deformation	• Difficult to achieve with small specimens • Samples must be homogeneous and geometrically consistent to eliminate risk of premature failure	*Unsuitable for mechanical analysis of specimens, due to sample size limitations and anisotropic nature of sinus bone*	[**7**] [**8**] [**9**] [**14**] [**11**]

ways. These include the incorporated use of load cells within the loaded structure [**15**], the external application of strain gauges to measure the resultant geometric variation of surgical tool handles with respect to applied force [**16**], and tactile sensors that measure grip forces directly from the hand. Applied force data can be used for direct comparison of real/synthesized bone samples. When deciding upon the most appropriate methodology a number of key requirements were taken into account, which are listed below:

(a) avoid interference with tools during routine operation;
(b) ease of use, with no complex pre-testing/calibration requirements;
(c) no extensive physical modification of tools;
(d) must be suitable for sterilization procedures, to enable potential *in vivo* surgical testing applications;
(e) transportable.

The most representative surgical instruments were identified before a procedure involving direct force measurement was established. Two primary types of forceps for bone removal in the sinus were selected; the Hijacs bone punch and through-cutting rongeurs. These instruments cover a range of procedures and multiple variants exist to enable access to the entire sinus complex.

To enable development of the experimental apparatus, a solid understanding of the mechanical actuation of these tools and their interaction with the sample at the contact head was critical. All of these instruments are based on the mechanical actuation of solid sections. The through-cutting rongeurs are shown in Fig. 5 and their basic functionality is explained.

Through-cutters, both the rongeurs and the punch, induce fracture along a given cutting line. These tools are used in the discrete removal of material in high-risk areas of the sinus. Specimens are subjected to high shear forces, similar to that of four-point bend testing, and typically fracture along or close to the cutting line, as illustrated in Fig. 6.

The rongeurs are typically used for the removal of bone up to 1 mm thick. Specimens that exceed 1 mm thickness will usually require the more substantial Hijacs bone punch. Following initial research on direct force measurement, recognition of a suitable engineering solution involving the use of strain gauges was deemed the least intrusive method available in determining the force applied to the instrument. Figure 7 demonstrates the principle and operation of the direct force measurement device. The entire direct force measurement system will be referred to as the force recognition surgical data logger (FRSDL).

The concept relies specifically on the measurement of strain in the tool arms when a resistance to cutting force is experienced. The force applied to these arms, in order to induce fracture of the test sample, will be proportional to the strain experienced by the arms. Strain gauges were used to quantify this variable, which was then correlated to force through subsequent calibration techniques. The Wheatstone bridge circuit requires a series of additional interface electronics in order to effectively amplify the output signal and convert it to a suitable form for laptop-based data logging.

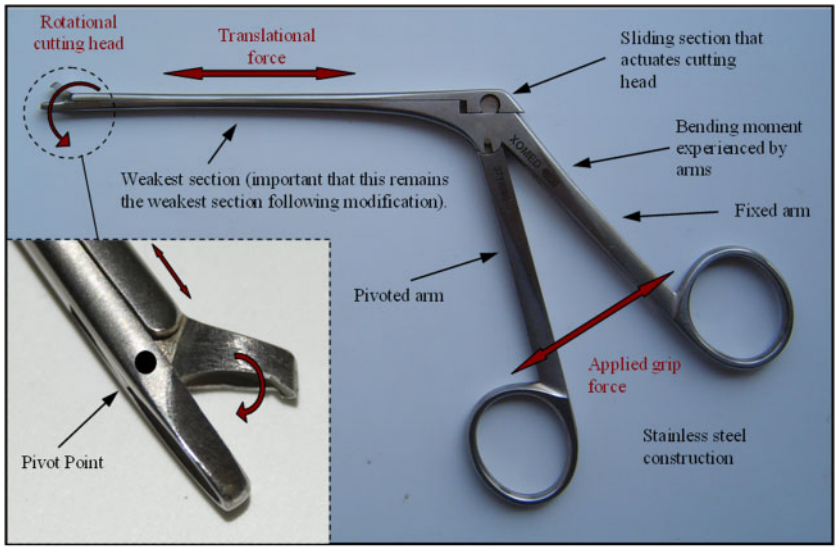

Fig. 5 Through-cutting rongeurs

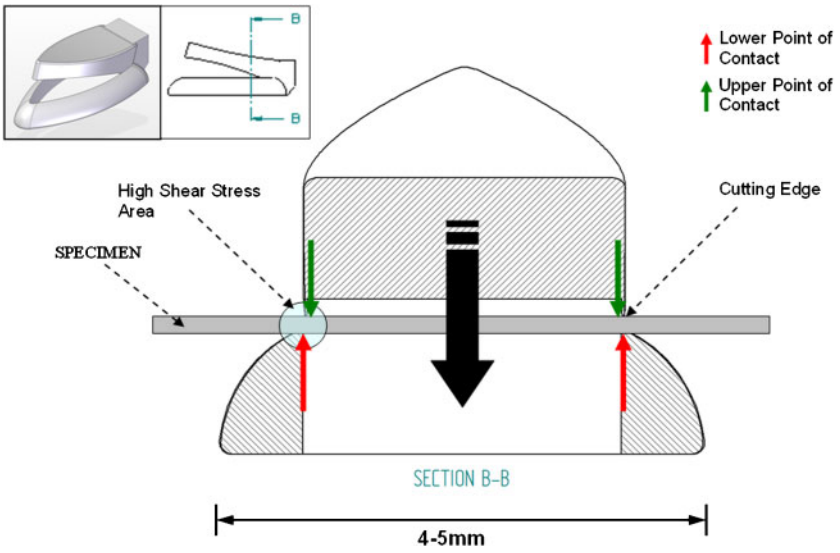

Fig. 6 Cross-section of through-cutting instrument head

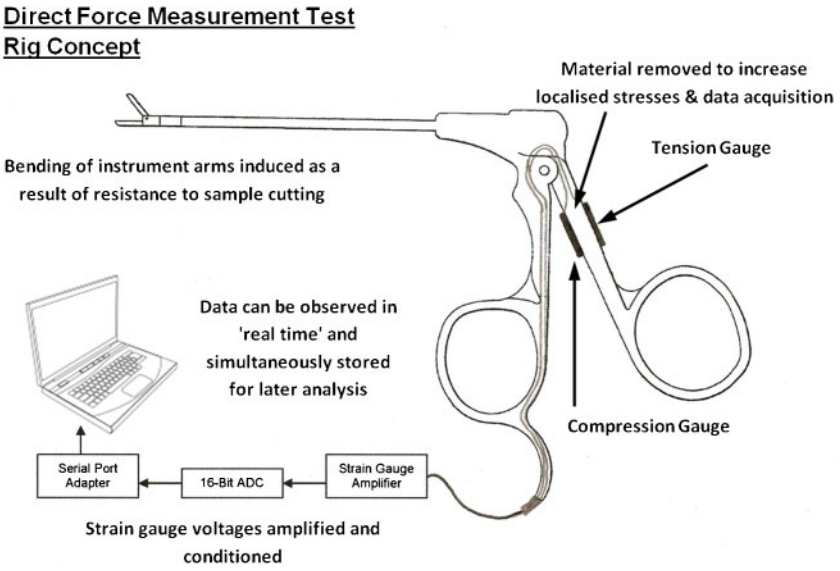

Fig. 7 Design of FRSDL

A bespoke program was written that controls the acquisition of data from the strain gauge system. Microsoft Visual Basic 6 controls communication between the personal computer (PC) and analogue-to-digital converter (ADC). The program enables the user to preselect a number of different sampling rates, control the influx of data from up to two tools simultaneously, and view current values in real time.

Once the sensitivity and range of the FRSDL had been verified through initial testing, calibration was conducted to establish the relationship between ADC output and applied force. Results demonstrated that it requires approximately 6.342 kg (62.22 N) of grip force to reach the full-scale output (FSO) of the FRSDL. Calibration showed excellent consistency throughout the entire force range, with sample noise not exceeding ± 6 bits, equivalent to ± 0.0145 V. Following calibration, this translates to an error of ± 0.0372 kg.

Calibration data demonstrated a close correlation between actual results and a corresponding linear approximation. Both lines coincided to the degree that the formula for the line of best fit could be taken as a close approximation of the measured data. Calibration provided the user with the ability to visualize material cutting characteristics in standard engineering units (SI), which is valuable for calculation and discussion purposes.

2.4 Data analysis

A series of continual modifications were made to the FRSDL instrument, which developed it from a single quarter bridge circuit to a full four-gauge bridge. This improved sensitivity and consistency of the results. In order to accelerate the process of data analysis, Visual Basic scripts were utilized within Microsoft Excel to provide a common analysis program for all data files. This eliminated laborious manual work associated with sequentially selecting each peak value, which cannot be automated through standard sorting functions in Excel.

Analysis of data within the program code involved the calculation of an average value from the entire data set. This was then used as a control value which is unique to that data set. From this value, upper and lower thresholds were automatically calculated. The program then sequentially compared the current value with each threshold and that of the previous value in order to determine whether this was a peak. Each peak value represented the maximum cutting force at fracture of the material tested and was used as the primary method of multiple sample comparison.

Mean, median, upper, and lower quartiles and the inter-quartile range of the peak values were calculated for each data set in order to analyse sample variation. Inter-quartile range was used as opposed to conventional range as this helped to reduce the effect of erroneous outlying values on final results.

Most erroneous results, due to tool-lockout or premature failure of the sample, were filtered out during sampling analysis of the data set. Unlike the total range, the inter-quartile range is a robust statistic and had a proportion of incorrect observations of less than 25 per cent, making it less susceptible to the effects of erroneous outliers. Inter-quartile range was used to quantify the repeatability and consistency of the test specimens produced.

2.5 Mechanical analysis of the cadaver sinus

Following μCT evaluation of the sinus block, further sectioning was conducted in order to gain access to the sinus for quantitative testing using the FRSDL. The sample block was sectioned vertically in order to prevent damage to either left or right sinuses, which also enabled the test to be performed in an orientation that was in keeping with surgical procedures.

Full access to each lateral half of the sinus also enabled full details of the cutting location and specimen geometry to be documented for cross-reference with numerical data at a later time. Figure 8 shows an internal view of the left portion of the sinus block on completion of the sectioning operation. Elements of the anatomical regions tested are identified in Figs 9 and 10.

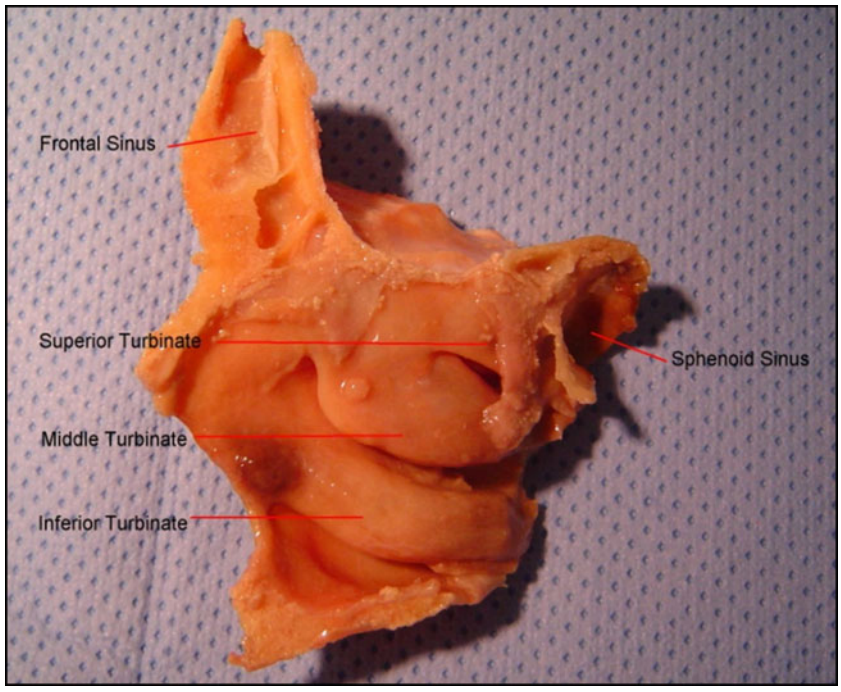

Fig. 8 Internal view of the sinus block section

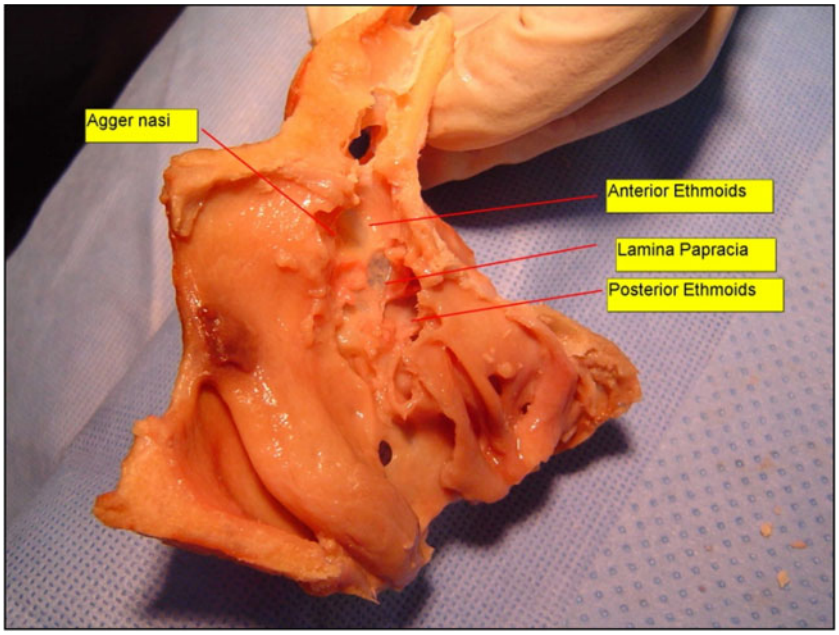

Fig. 9 Anatomical test regions 1

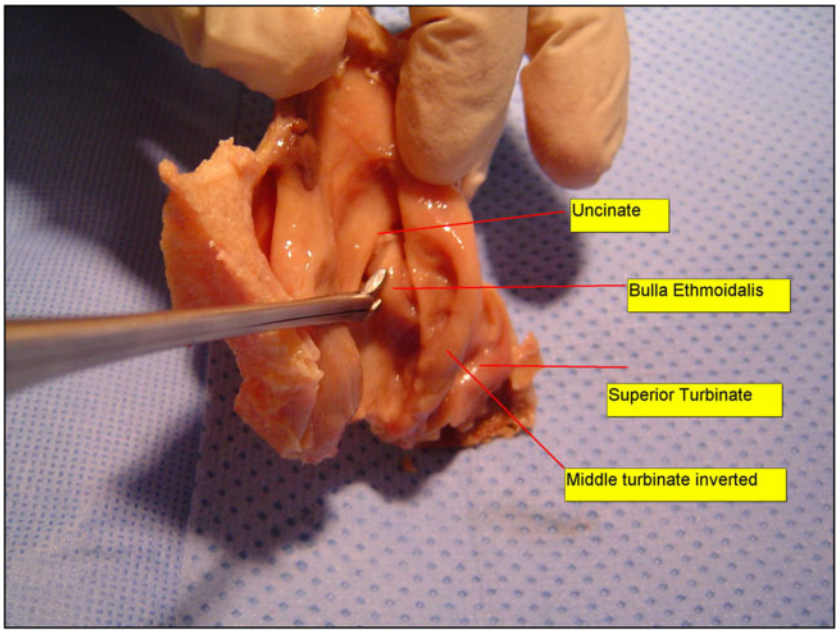

Fig. 10 Anatomical test regions 2

2.6 3D printing test specimen design and infiltration

In order to identify an initial target range, a series of scoping experiments was conducted. This also provided verification of the functionality of the FRSDL and ensured its operation within the required range of sensitivity and accuracy.

A selection of samples was produced with various infiltrants in order to provide a range of physical properties for assessment. These samples were then dissected by the clinical partners using the surgical tooling. This initial clinical qualification informed that the mechanical behaviour of the range of bone varieties in the human sinus lay somewhere between uninfiltrated 3DP samples (at the lower extent) and cyanoacrylate (at the upper extent).

An experimental sample design was then produced that reflected the relevant thicknesses derived from the CT data. The test specimen geometry was designed using CAD. Figure 11 shows the test

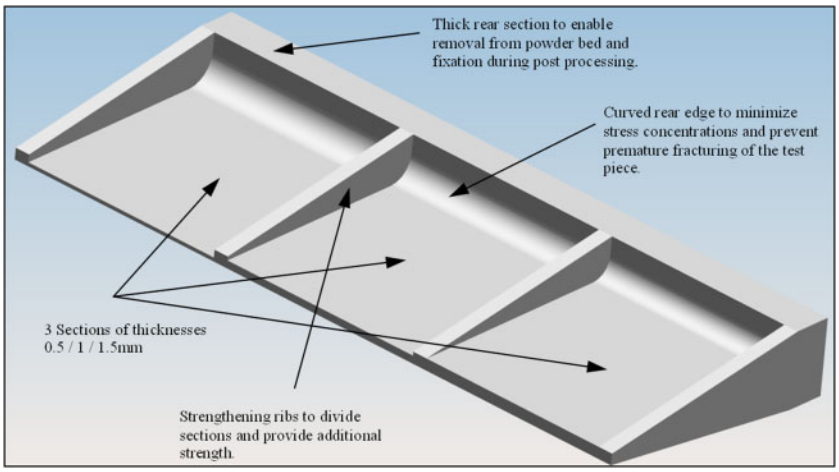

Fig. 11 CAD model of 3DP experimental test specimen

specimen design and highlights some of the key features.

Utilizing the prior clinical qualified input as guidance to relevant physical property extremes, a range of infiltrants was identified for experimentation. The softest sample would be tested in a purely 'green' uninfiltrated state to provide a low value for comparison purposes, while the hardest sample would be infiltrated with cyanoacrylate. Three infiltration techniques were adopted for the specimens used in this work, whereby the infiltration method was chosen in relation to material viscosity and availability. Immersion was conducted at ambient temperature except in the case of paraffin wax which required an elevated temperature of 60–70 °C. Parts were immersed for 30 s before being removed and placed in a drying orientation that encouraged 'run-off' of excess material. A spray vapour application technique was adopted for polyvinyl alcohol (PVA) in order to prevent saturation of the specimen, which leads to loss of geometric features. Finally, a physical surface application methodology was adopted for materials that were unsuitable for immersion or difficult to work with, in the quantities required for immersion, for example cyanoacrylate.

The full list of the infiltration materials analysed is detailed in Table 2. These infiltrant materials were examined in isolation and as mixtures. They were also investigated with infiltration in multiple phases. In the results section, infiltration materials testing conducted is presented using two symbols. The '&' sign symbolizes a mixture of these materials are produced and infiltrated in unison; the '+' symbolizes the sequential infiltration of materials following curing and drying periods. The notation PVA 1,2,3, and 4 refers to a series of infiltration techniques used and represent immersion, surface application, vapour, and vapour and surface application respectively. All parts were produced on a Z-Corporation 510 machine using Zp130 powder.

3 RESULTS

3.1 Cadaver testing

Results of cadaver testing are summarized in Tables 3 and 4, and Fig. 12.

Table 2 Infiltration material summary

Infiltration material	Constituents	Application method	Reference name
Paraffin wax	100% paraffin	Immersion	Wax
Polyvinyl alcohol	—	Vapour / immersion	PVA
Cyanoacrylate	Methyl-2-cyanoacrylate, ethyl-2-cyanoacrylate	Surface application	CY
Epoxy resin	Epichlorohydrin, bisphenol A	Surface application	Epoxy
Polyurethanes	Cobalt 2- ethylhexanoate, ethyl methyl ketoxine, three different formulations	Immersion	PU 1 PU 2 PU 3
Acetate	Tosylamide-formaldehyde mixed with butyl acetate or ethyl acetate	Immersion	Acetate
Cellulose	Cellulose or a cross-linkable polyester in a suitable solvent	Immersion	Cellulose
Shellac	Natural shellac	Surface application	Shellac

Table 3 Summary of through-cutter cadaver testing

	Through-cutter			
Anatomical region	Sample thickness (mm)	Average peak force (N)	Sample variation (N)	Cuts performed
Anterior ethmoids	0.3	4.4	0.22	3
Bulla ethmoidallis	0.5	6.9	1.74	9
Laminar papracia	0.2	9.9	1.3	8
Middle turbinate small	$0.2 < x < 0.8$	12.11	2.55	7
Posterior ethmoid	0.1	13.6	2.61	9
Medial wall maxillary small	$0.2 < x < 0.275$	14.52	1.44	4
Uncinate	0.2	16.74	2.49	5
Middle turbinate medium	$0.8 < x < 1.3$	17.86	1.55	4
Medial wall maxillary large	$0.275 < x < 0.35$	21.91	4.61	4
Superior turbinate	0.4	23.45	0.56	3
Middle turbinate large	$1.3 < x < 1.8$	27.94	2.55	4
Orbit floor	—	45.36	2.45	6
Geometric range tested (mm)		1.7		
Force range recorded (N)		40.96		
% of FSO detectable force range (0–62 N)		66.06%		

Table 4 Summary of Hijacs bone punch cadaver testing

	Hijacs bone punch			
Anatomical region	Sample thickness (mm)	Average peak force (N)	Sample variation (N)	Cuts performed
Agger nasi 1	0.45	51.82	2.86	5
Agger nasi 2	0.45	57.06	0.19	2
Geometric range tested (mm)		0		
Force range recorded (N)		5.24		

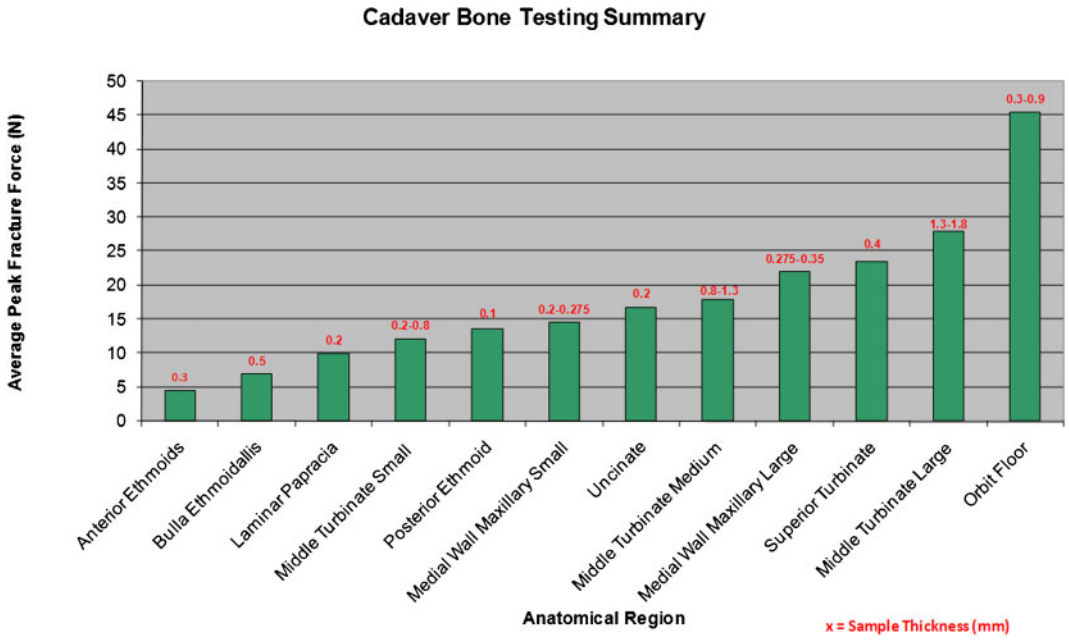

Fig. 12 Summary of cadaver bone testing

3.2 Phantom testing

Results of phantom testing are summarized in Fig. 13.

4 DISCUSSION

The mechanical testing of the cadaver provided a spectrum of results to which synthetic 3DP materials could be compared. Results obtained from the middle turbinate and medial wall maxillary demonstrated the problems associated with geometric variation throughout the sinus. For example, 15 cuts were performed on the middle turbinate, which varied in thickness from 0.2 to 1.8 mm. This resulted in a highly varied raw data set. In order to effectively define the cutting force required to fracture these different bone thicknesses, the data were subsequently split into three subcategories that divided the effective geometric variation into suitable data sets. Each data set was then subsequently analysed in order to quantify the average cutting force and sample variation.

Following quantification of the cutting characteristics of cadaver sinus bone, experiments were conducted in order to explore a broad range of 3DP specimens produced using different infiltrant materials. The objective was to discover a series of materials that would represent a substantial relevant range of properties representing those found in prior testing of the sinus. This would allow the ongoing refinement of the exacting properties of key materials at a later date. This work incorporated the use of multiple infiltrant materials in two key ways: first, the amalgamation of materials in their liquid form, prior to infiltration, and second the exploration of multistage processes, separated by curing and drying periods.

Many materials reacted poorly when mixed in their raw form, usually separating into an inconsistent mixture of reacted and unreacted compounds. The only materials that could be successfully combined into a suitable fluid were polyurethanes, polishes, and suspended cellulose/polyesters (hardeners).

Multistage infiltration techniques were used when material selection inhibited the combination of multiple substances prior to infiltration. Allowing sequential infiltration operations to cure fully before application of further materials prevented the reaction of multiple substances caused by simultaneous curing. The main drawback to this method is the consideration that later infiltration materials could simply create a surface coating on the test specimen, as opposed to a true infiltrant, which is absorbed into the structure.

Modifications to the surgical devices have deliberately been minimal and non-invasive in order to

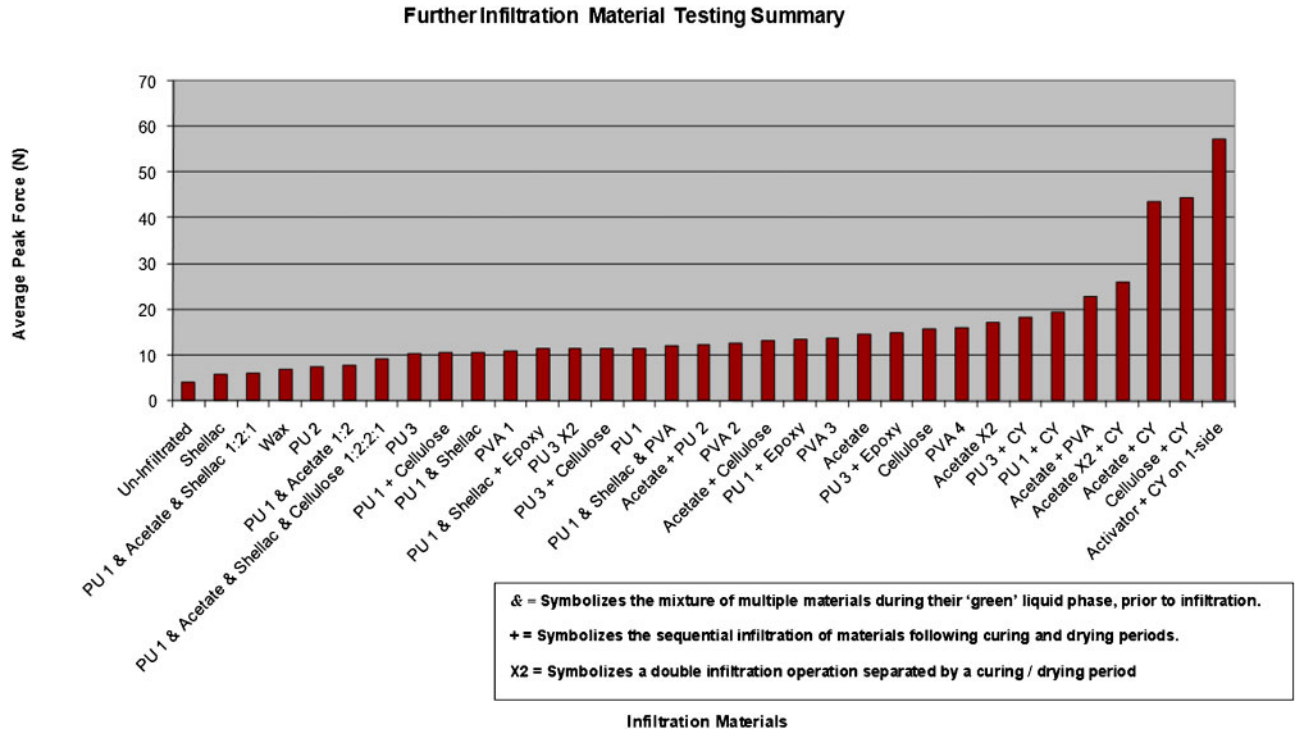

Fig. 13 Summary of phantom testing

safeguard operation of the instrument and prevent interference with the working practices of surgeons using these devices. The use of a singular device for both cadaver and 3DP testing has reduced potential comparison issues.

Different degrees of success have been experienced according to the nature and method of infiltration. It became clear at an early stage during this project that water-based infiltrant materials are not entirely suited to infiltration of delicate intricate 3DP structures, owing to the water-based nature of the binder material used in their construction. This work indicates that spirit-based polyurethanes and acrylics present the most potential for infiltration. The advantages of using immersion techniques must also be emphasized as they provide a more consistent method of infiltration when compared with drip, paint, or spray techniques. Immersion techniques will also enable infiltration of hidden details and cavities within the structure that are otherwise inaccessible.

The depth of infiltrant penetration was seen to be highly influential on resultant properties. This can be controlled through the use of two-stage infiltration, whereby a filler material such as hardener or varnish is used initially to strengthen the structure and decrease porosity, followed by infiltration with a harder material such as cyanoacrylate. Suspended cellulose/polyesters (hardeners) were found to be very effective at initially strengthening parts while leaving sufficient porosity for further infiltration to take place. It can be seen from these results that as the parts' ability to absorb material decreased through use of high-viscosity first-stage infiltrants, the penetration depth of second stage materials was also limited.

The ability to manipulate dual physicality within a single article could be particularly exploited in other forms of bone surgery simulation. Producing a softer inner core accompanied by a hard outer layer corresponds with the cancellous–cortical relationship evident in other bone structures.

The use of μCT has successfully provided higher-resolution imaging of the sinus complex, providing indication of the tissue relationships within the thin-walled ethmoid complex. Limited power outputs and field-of-view restrictions prevent clinical CT systems from matching this resolution. Higher-resolution scans could be achieved through further μCT analysis; however, in order to achieve the 10 μm resolutions that μCT is capable of, sample sizes would need to be greatly reduced, which would prevent characterization of the entire sinus block simultaneously.

5 CONCLUSION

Use of the direct force measurement technique has enabled quantification of cutting characteristics from the human sinus in a range of anatomical locations. Through modification of existing instrumentation, issues of sample size, preparation requirements, and logistics have been resolved. The FRSDL system enables real-time data acquisition combined with true mobility. Through use of this equipment, quantitative data have been generated on the cutting characteristics and strength of cadaver sinus bone. The same process has then been successfully implemented in the quantification of synthesized 3DP samples, infiltrated using a range of materials and techniques. Accurate comparison of cutting forces relies on the principle of using the same equipment and procedures for all tests conducted. Direct force measurement of real surgical devices addresses this, while also opening up a range of possibilities with regard to the testing and analysis of living tissue during surgery.

This work has shown that a wide range of properties can be achieved according to selection and methodology of infiltration. Importantly, this range encompasses the properties of sinus bone determined through quantitative testing and shows that 3DP is a highly capable and flexible technique for producing physically representative surgery simulation phantoms of the human sinus. This research also illustrates great potential for extending this work into other clinical fields.

ACKNOWLEDGEMENTS

The authors would like to acknowledge the funding of the Engineering and Physical Sciences Research Council (EPSRC) (IMCRC 223) and the support of the companies of Z-Corporation and Let's Face It.

REFERENCES

1 **Hieu, L. C., Zlatov, N., Sloten, F. V., Bohez, E., Khanh, L., Binh, P. H., Oris, P.,** and **Toshev, Y.** Medical rapid prototyping applications and methods. *Assembly Autom.*, 2005, **25**(4), 284–292.

2 **Savalani, M. M., Hao, L., Zhang, Y., Tanner, K. E.,** and **Harris, R. A.** Fabrication of porous bioactive structures using the selective laser sintering technique. *Proc. IMechE, Part H: J. Engng in Medicine*, 2007, **221**(8), 873–886. DOI: 10.1243/09544119JEIM232.

3 Z-Corporation, further details available from http://www.zcorp.com/.

4 **Chua, C. K., Leong, K. F.,** and **Lim, C. S.** *Rapid prototyping – principles and applications*, 2003

(World Scientific Publishing Co.) (ISBN 981-238-117-1).

5 **Ruegsegger, P., Koller, B.,** and **Muller, R.** A microtomographic system for the nondestructive evaluation of bone architecture. *Calcified Tissue Int.*, 1996, **58**(1), 24–29.

6 **Postnov, A. A., Zarowski, A., De Clerck, N., Vanpoucke, F., Offeciers, F., Van Dyck, D.,** and **Peeters, S.** High resolution micro-CT scanning as an innovatory tool for evaluation of surgical positioning of cochlear implant electrodes. *Acta Oto-Laryngologica*, 2006, **126**(5), 467–474.

7 **Cowin, S. C.** *Bone mechanics handbook,* 2nd edition, 2001, ISBN 0-8493-9117-2 (CRC Press, Boca Raton, Florida).

8 **Fini, M., Cadossi, R., Cane, V., Cavani, F., Giavaresi, G., Krajewski, A., Martini, L., Aldini, N. N., Ravaglioli, A., Rimondini, L., Torricelli, P.,** and **Giardino, R.** The effect of pulsed electromagnetic fields on the osteointegration of hydroxyapatite implants in cancellous bone: a morphologic and microstructural *in vivo* study. *J. Orthop. Res.*, 2002, **20**, 756–763.

9 **Ziv, V., Wagner, H. D.,** and **Weiner, S.** Microstructure–microhardness relations in parallel-fibered and lamellar bone. *Bone*, 1996, **18**(5), 417–428.

10 **Yuehuei, H.** and **Draughn, R. A.** *Mechanical testing of bone and the bone implant interface*, 2000 (CRC Press, Boca Raton, Florida) (ISBN 0-8493-0266-8).

11 **Shahar, R., Zaslansky, P., Barak, M., Friesem, A. A., Currey, J. D.,** and **Weiner, S.** Anisotropic Poisson's ratio and compression modulus of cortical bone determined by speckle interferometry. *J. Biomechanics*, 2007, **40**, 252–264.

12 **Wallace, J. M., Rajachar, R. M., Chen, X., Shi, S., Allen, M. R., Bloomfield, S. A., Les, C. M., Robey, P. G., Young, M. F.,** and **Kohn, D. H.** The mechanical phenotype of biglycan-deficient mice is bone- and gender-specific. *Bone*, 2006, **39**, 106–116.

13 Bose Corporation. Micromechanical multicyclic creep tests of human cortical bone, internal document (ElectroForce® Systems Group, Bose Corporation, Eden Prairie, Minnesota, USA).

14 **Zeung, Y., Sun, X., Yang, J., Wu, W., Xu, X.,** and **Yan, Y.** Mechanical properties of nasal fascia and periosteum. *Clini. Biomechanics*, 2003, **18**, 760–764.

15 **Tingelhoff, K., Wagner, I., Eichhorn, K., Rilk, M., Westphal, R., Wahl, F. M.,** and **Bootz, F.** Sensor-based force measurement during FESS for robot assisted surgery. GMS CURAC, internal document, 2007, Doc02.

16 **Hanna, G. B., Drew, T., Arnold, G., Fakhry, M.,** and **Cuschieri, A.** Development of force measurement system for clinical use in minimal access surgery. *Surg. Endoscopy*, 2008, **22**(2), 467–471.